We are IntechOpen, the world's leading publisher of Open Access books Built by scientists, for scientists

6,900
Open access books available

185,000
International authors and editors

200M
Downloads

Our authors are among the

154
Countries delivered to

TOP 1%
most cited scientists

12.2%
Contributors from top 500 universities



WEB OF SCIENCE™

Selection of our books indexed in the Book Citation Index in Web of Science™ Core Collection (BKCI)

Interested in publishing with us?
Contact book.department@intechopen.com

Numbers displayed above are based on latest data collected.
For more information visit www.intechopen.com



Chapter 8

Geoelectrical Sounding and Imaging over the Central Zone of Panama

Alexis Mojica

Additional information is available at the end of the chapter

http://dx.doi.org/10.5772/intechopen.74210

Abstract

Electrical properties of rocks and geoelectrical resistivity method have been discussed in this chapter, in which the results of an electrical survey over the sedimentary terrain of the central zone of Panama (Central America) are presented. This study therefore includes (i) a petrophysical study with the aim of relating its electrical resistivity values with the volumetric water contents, (ii) an electrical resistivity imaging (2D inversion), and (iii) an electrical sounding (1D inversion) for detecting the water table and its corresponding stratigraphy and variation with time. Two datasets for these last methods have been developed with the aim of monitoring the percentage changes in model resistivity. Petrophysical tests show good fits between resistivity and volumetric water content and known parameters for rocks and soils. 1D and 2D inversions show a significant reliability with the stratigraphic information obtained from a borehole and strong changes caused by rainy season in this tropical zone.

Keywords: electrical sounding, electrical resistivity imaging, petrophysical, sedimentary rocks, geophysical inversion, time-lapse imaging

1. Introduction

In geophysical studies, resistivity method can be used in fault zone detection and stratigraphic characterization, in hydrology for tracing water transport during a given period of irrigation studies, and for archeological and agriculture purposes. Resistivity is controlled by water content, soil texture and its geochemical properties, lithology, organic matter content, and thermodynamic parameters. The electrical properties of the materials that make up part of the outermost layers of the crust can be studied either electrically or electromagnetically from the response produced by the flow of electrical current in the subsurface. Geoelectrical methods

IntechOpen

© 2018 The Author(s). Licensee IntechOpen. This chapter is distributed under the terms of the Creative Commons Attribution License (http://creativecommons.org/licenses/by/3.0), which permits unrestricted use, distribution, and reproduction in any medium, provided the original work is properly cited. CC BY

take into account these electrical and electromagnetic aspects whose physical parameters, such as electrical current, electrical potential, and electromagnetic fields can be measured naturally or artificially. In 1830 a self-potential method based on the natural electrical response of the subsurface was used [1]. In his work, low-intensity electrical currents generated by some minerals were identified. Later, this methodology underwent certain changes in terms of using a natural source, and Schlumberger, during the second decade of the last century, decided to use artificial sources by injecting electrical current into the subsoil.

The electrical resistivity of rocks is a physical property that is characterized by very large variations in their values; most rocks and soil can be classified as highly resistive or insulating, and only metallic minerals and some of their salts can be classified as conductors. There are three ways in which electrical current can propagate through the subsurface: ohmic or electronic, electrolytic, and dielectric. The first is related to normal type of flow of charges through materials with free electrons such as metals; for electrolytic conduction, almost all soils and rocks have pores that could be saturated with water; thus, for those types of soils and rocks that have high ranges of electrical resistivity, the circulation of electrical current is carried out exclusively through electrolytic conduction due to the presence of water contained in the pores and fissures of the material. This means that the value of the electrical resistivity depends on the concentration and degree of dissociation and mobility of ions [2]. Electrolytic conduction is produced by the slow movement of the ions within the electrolyte; therefore, the rocks are electrolytic conductors where the flow of electrical charge occurs through the conduction of ions. Dielectric conduction occurs only in materials with high electrical resistivity (insulators). According to [3], in this class of materials, the electrons can experience a slight displacement with respect to their atomic nucleus in the presence of a variable external electric field.

Geoelectrical methods include a wide variety of techniques that are adapted to the objectives of the investigation, the dimensions and topography of the area of interest, and the electrical properties of the soil and rocks that make up the study area and whether these properties undergo large variations. Techniques such as self-potential, telluric and magnetotellurics, electrical resistivity (which we will deal with in more detail in this chapter), electromagnetism, and induced polarization allow a rapid measurement of the electrical properties of the soil, such as electrical resistivity, or its opposite, electrical conductivity. These noninvasive techniques essentially involve the interpretation of these physical parameters of the soil, which quantify the degree of difficulty or ease in which a certain volume of soil responds to the passing of electric charges, respectively; for more details about these methods, see [1, 3–7].

The electrical resistivity method is one of the most common geoelectrical methods for the prior evaluation of soil in civil, environmental, archeological, geological, and agricultural projects. Its noninvasive nature and the rapid data acquisition make this method an inexpensive and effective tool in the detailed evaluation of soil. Then, the determination of the geochemical and geophysical properties of soil is essential to the development of civil and agricultural engineering projects. In archeology, for example, the resistivity method constitutes an additional tool of remarkable value when evaluating in advance the presence and/or absence of buried archeological features, thus optimizing resources and time spent in the field, with significant economic impact. Conventional methods of soil analysis directly affect the soil because the samples must be taken and analyzed in a laboratory.

http://dx.doi.org/10.5772/intechopen.74210

Geoelectrical methods have been used extensively in groundwater studies and stratigraphic characterization. Several authors have carried out studies of samples in the laboratory using petrophysical relationships [8] in which the volumetric water content is obtained by the measurement of dry bulk density and the gravimetric water content, for example, see [9, 10] in leachate recirculation studies, [11, 12] for root-zone moisture interactions and watershed characterization, and [13] in rainfall simulations.

This chapter gives a short description of electrical properties of rocks, basic principles of the geoelectrical resistivity method, and a case study of sedimentary rocks of central zone of Panama (Central America) that include petrophysical soil analysis and 1D and 2D inversion methodology. This study has been developed with the aim: (i) to obtain a relationship between electrical resistivity with volumetric water content and correlation with the empirical equation of Archie's law and (ii) to define a 1D and 2D electrical models for two datasets obtained in different seasons (dry and rainy) and relate the results to the stratigraphy and in addition monitor the percentage changes of calculated resistivity values.

2. Study area and geology

The study area is located in an open test zone of the extension of the Technological University of Panama, 19 km East-Northeast of Panama City in the central zone of Isthmus of Panama, Central America; see **Figure 1(a)**. Panama has a rainy and dry seasons, with a tropical maritime

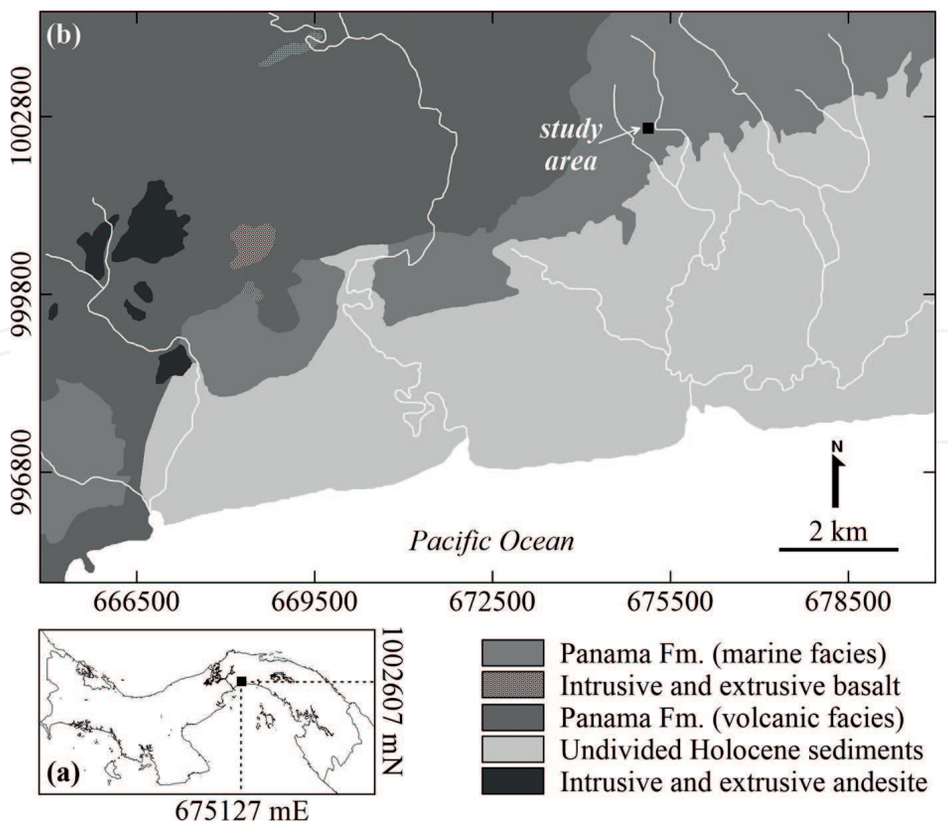


Figure 1. (a) Location map and (b) geological setting of study area and environs [18].

climate with a hot, humid, rainy season (May → December) and a short dry season (January → May). According to [14] the transition at the end of the dry season to the beginning of rainy season is linked with the disappearance of trade winds.

According to [15–18], the study area is characterized by a dense sequence of sediments and volcanic rocks. The site is influenced by the geological elements of the Panama Formation (marine facies) of early to late Oligocene; these elements consist of tuffaceous sandstone, tuffaceous siltstone, and algal and foraminiferal limestone [18]. **Figure 1(b)** shows the geological map and study area and environs.

3. Methodology

3.1. Site layout and profile

To obtain a distribution of electrical resistivity values in lateral and vertical directions, and its variations for a period of three and half months, we have defined a North-South profile of 47 m long; this profile is superimposed on a borehole drilled in 2011 with a piezometer to monitor groundwater dynamics linked with dry and wet seasons. **Figure 2(a)** and **(b)** show the area with profile, electrical sounding, and borehole positions and **Figure 2(c)** a geotechnical scheme of the borehole.

3.2. Petrophysical relationship

A total of five soil samples were collected from the site to a depth of 20 cm. To obtain a relationship between resistivity and volumetric water content, we have used the ASTM standard G57-06, where the samples are homogenized inside a box of insulating materials as shown in **Figure 3**.

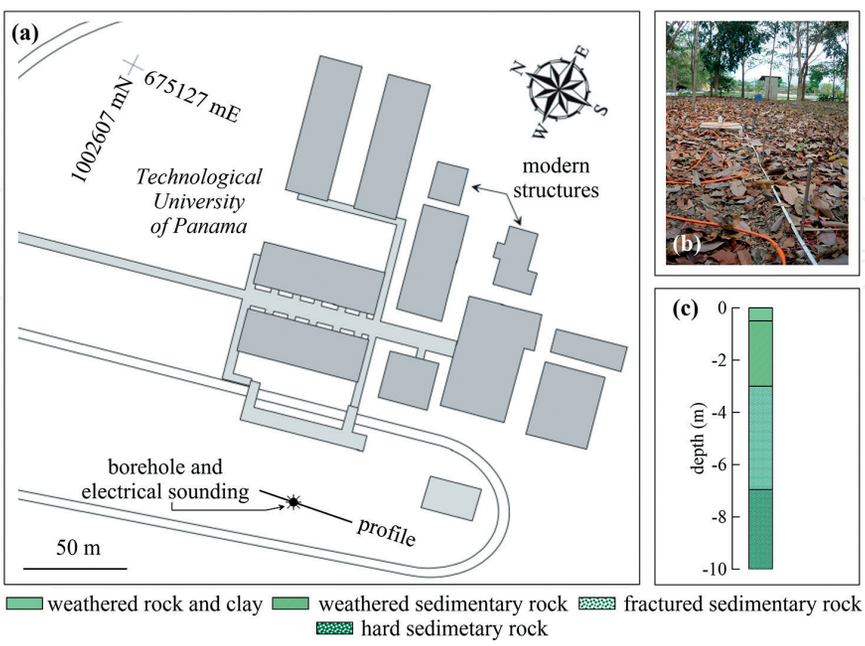


Figure 2. (a) Details of the study area with North-South profile and electrical sounding and borehole location, (b) panoramic of the field site, and (c) description of borehole log.

http://dx.doi.org/10.5772/intechopen.74210



Figure 3. LandMapper of Landviser and Miller soil box used for the measurement of the electrical resistivity of each soil sample in laboratory, according to ASTM standard G57-06 (photo courtesy of 3P Soc. Ltda).

In this box, two metal plates with an equal surface (S) are placed; we connected these plates to the source of electrical current or resistivity meter; see **Figure 3**. On the surface of the soil sample, two metal pins are inserted and separated by distance (l) to measure the voltage generated when the electric current passes through this sample. The value of electrical resistivity (ϱ) of the soil sample is given by:

$$\rho = RS/l \tag{1}$$

where R is the electrical resistance (in Ω). Volumetric water content (θ) and dry bulk density were obtained by weight difference (dried at 105°C for 24 hours) and calculating the gravimetric water content. The relationship between ϱ-θ of these samples can be demonstrated and then fit it into Archie's law [8]:

$$\rho = a\rho_w \Phi^{-m} S_a^{-n} \tag{2}$$

where a is the tortuosity factor, ρ_w is the electrical resistivity of the fluid filling the pores, Φ is the porosity (volume of void-space/bulk volume of the soil), S_a is the saturation of the sample (volume of fluid/volume of void-space), and m and n correspond to the cementation and saturation exponents of the rock, respectively. Under certain special conditions, it is possible to approximate these last parameters and to obtain the volumetric water content from Φ and S_a.

3.3. Electrical sounding and 2D electrical resistivity imaging acquisition and processing

The electrical resistivity methods generate three-dimensional patterns of electric current and electric potential flows within the subsurface [19]. In the case of two electrodes inserted in the surface of a homogeneous and isotropic half soil and separated by a short distance, it is possible to see a symmetrical pattern in the equipotential lines and in the electric flow lines; this means that at any point in the vicinity of the system, the electrical potential can be affected by the current electrodes (*A* and *B*). In situ, the voltage (ΔV) between two points (*M* and *N*) due to the two electrical sources is measured, and the electrical resistivity value is given by:

$$\rho = k \Delta V / i \tag{3}$$

where *k* corresponds to geometrical factor, which only depends on electrode position and *i* the electrical current.

In the case of an inhomogeneous medium, the measurements of the electrical resistivity of the subsurface tend to change when the set of four electrodes or quadrupole is moved along a profile. Another important aspect is that the value of electrical resistivity defined in the last equation will depend on the geometrical configuration of the electrodes and not on the intensity of the electric current. Therefore, the value obtained in this equation will correspond to a kind of average values of resistivity of the subsurface, from which we get the apparent electrical resistivity (ρ_a). It is important to note that the value of the apparent electrical resistivity of the soil will be its real value only if the soil is homogeneous. In practice there are different types of quadrupole arrays whose use will depend on the objectives of the research. Each of them is characterized by different geometric constants (*k*); **Figure 4** presents the most common arrangements used in soil exploration.

For each of the linear arrays of **Figure 4**, the record of the apparent electrical resistivity value of the subsoil is taken at the center of the internal electrodes; the measurement point is located at the center of the four electrodes. These quadrupole arrays allow the development of several modalities which are closely related to the objectives of the research. In this work we used the electrical sounding and 2D electrical resistivity imaging. The first method consists of keeping the position of the potential electrodes fixed (1 m apart for this study) and moving the current electrodes by 1 m. This procedure, illustrated in **Figure 5(a)**, allows defining a tabular model of the subsurface based on the geometrical distribution of the strata that have different electrical properties.

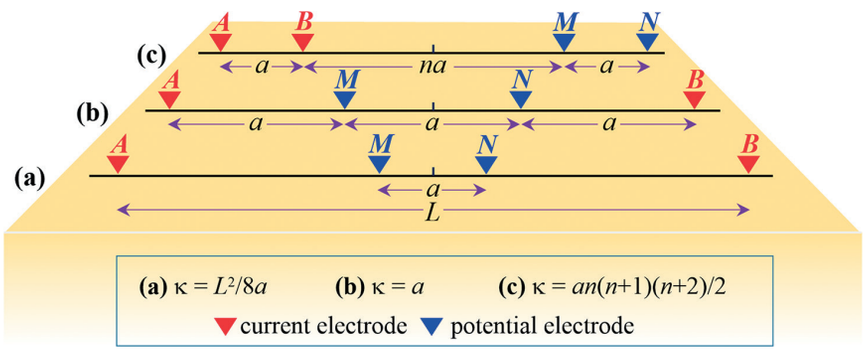


Figure 4. Some common quadrupole arrays: (a) Schlumberger, (b) Wenner, and (c) dipole–dipole and geometric constant.

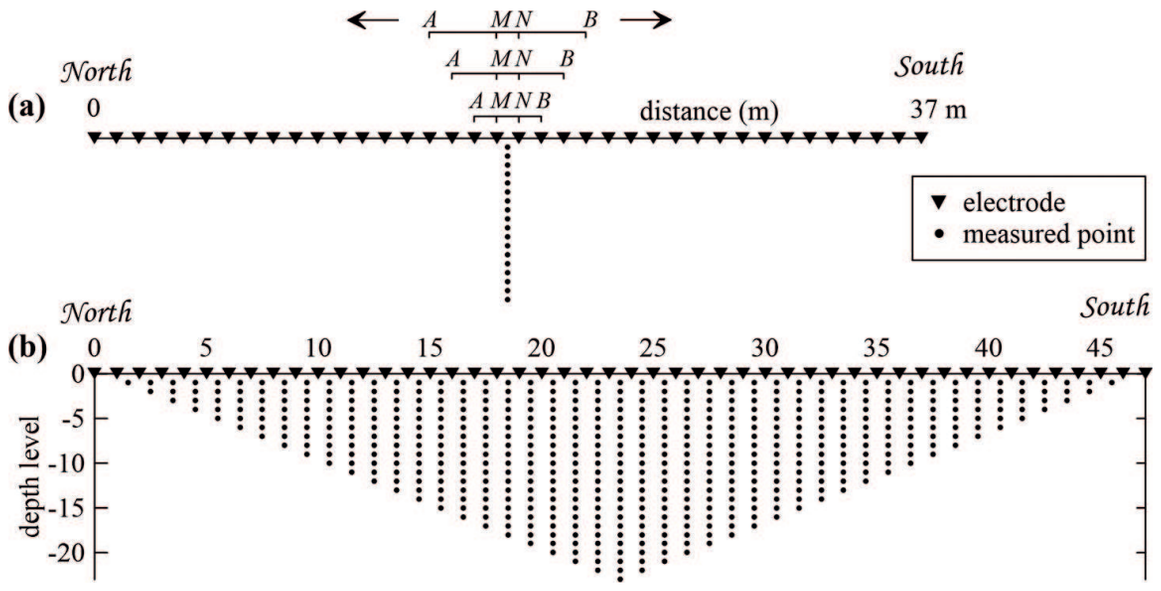


Figure 5. Distribution of apparent electrical resistivity data points for (a) the electrical sounding with a Schlumberger array and (b) a pseudo-section for imaging analysis with a Wenner-Schlumberger array.

The apparent resistivity value corresponding to each distance AB/2 is plotted logarithmically, resulting in a curvilinear tendency and, subsequently, with the resolution of the 1D inverse problem. This dataset is fitted to a curve that obeys the number of layers with their respective values of calculated electrical resistivity and thickness. The aim of inverse problem is to reconstruct a model from apparent electrical resistivity values. Two resistivity datasets were collected using a Schlumberger electrode configuration on the 16th of February, 2012, and 31st of May, 2012.

The second method consists of obtaining a high-resolution 2D image of the distribution of the electrical resistivity both laterally and vertically. The process consists of obtaining a set of apparent electrical resistivity values through a finite number of electrodes aligned along a profile with a constant distance between them (1 m for this study). The data can be obtained by varying the distances between the pairs of transmitter-receiver electrodes by multiples of a value with a computer-controlled multielectrode system. **Figure 5(b)** shows the electrode location along the profile and the measured points.

Measurements (for electrical sounding and 2D electrical resistivity imaging) were performed with a Syscal R1 Switch-48 (IRIS Instruments), in a simple mode for the first and a multielectrode mode for the second. In respect of the acquisition setting, the maximum value allowed standard deviation of the measurement was fixed at 1%; minimum and maximum number of stacks per measurement and the current time per cycle were fixed at 3 and 6 and 500 ms, respectively. To obtain a realistic 2D image of electrical resistivity distribution in the soil, we used a cell-based inversion method; this method subdivided the subsurface into a number of rectangular cells whose positions and sizes can be fixed [20]. The aim is to use an inversion algorithm to calculate the electrical resistivity of the cells that provides a model response that agrees with the apparent electrical resistivity values obtained in the field. In this study we used the regularized least-square optimization method [20–22]. This optimization method has two different constraints: the smoothness-constrained method [21] and the robust method [23]; the first is used when the subsurface exhibits a smooth variation in resistivity distribution and the second in regions that are piecewise constant and separated by sharp boundaries [20, 24].

As in the electrical sounding, two resistivity datasets were collected using a Wenner-Schlumberger array for the electrical resistivity imaging on the 16th of February, 2012, and 31st of May, 2012.

3.4. Time-lapse inversion

To monitor the changes in subsurface resistivity values during the period defined in the study area, we used the Res2Dinv inversion software (Geotomo); the time-lapse dataset can be interpreted through the time-lapse method proposed by [25]. In this software, the initial dataset for the inversion model is used as a reference model in the inversion of the later time-lapse datasets [26]. For our first dataset, we used the robust method; regarding another inversion parameter, we used an initial damping factor of 0.15, minimum damping factor = 0.030, and a simultaneous inversion.

4. Results and interpretation

4.1. Resistivity: volumetric water content derived from soil samples

Figure 6 presents a plot of electrical resistivity versus the volumetric water content of the soil samples obtained in the surveyed area. The fit was done using a power function with a good coefficient of determination, R^2 of 0.950; high values of resistivity of this type of soil (weathered rock) can be linked to 26% of volumetric water content, while the low values of electrical resistivity of the samples are related to 49% of water content.

4.2. Electrical sounding

Figure 7(a) represents the two datasets obtained with a Schlumberger array in the given periods; subsequently, with the resolution of the inverse problem 1D, these datasets were fitted to a curve (for each one) that obeys the number of layers with their respective values

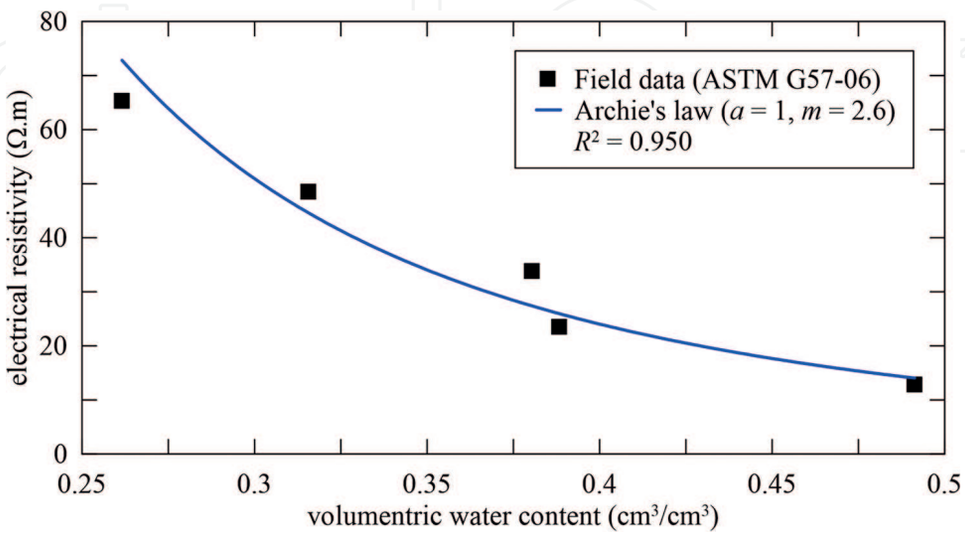


Figure 6. Relationship between the electrical resistivity and the volumetric water content obtained in the surveyed area.

http://dx.doi.org/10.5772/intechopen.74210

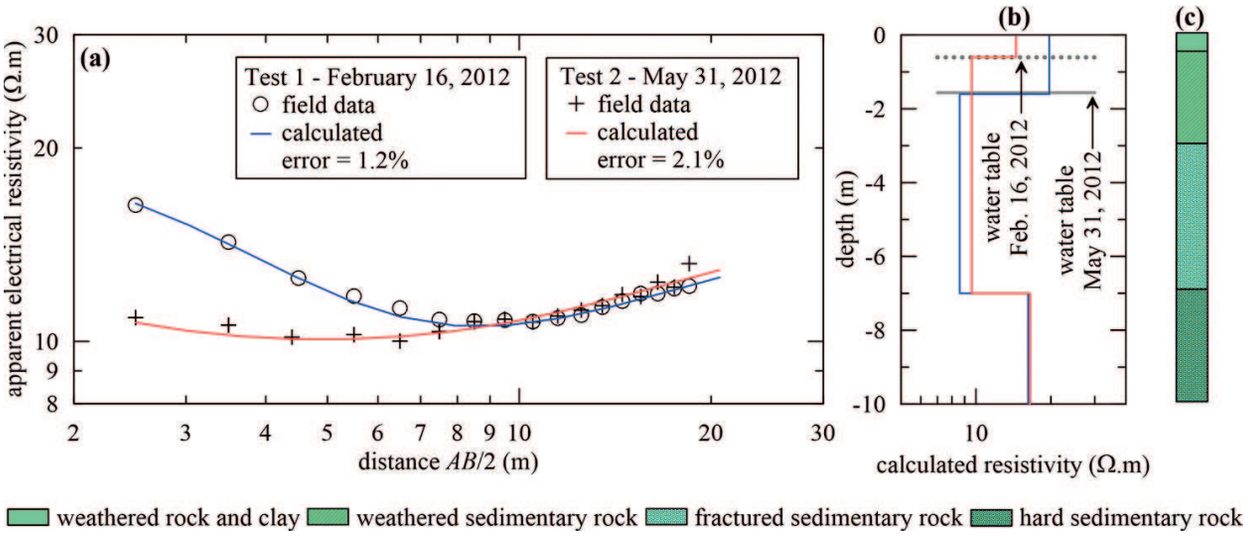


Figure 7. (a) Logarithmic representation of the two datasets as a function of distance AB/2, (b) tabular earth model obtained from the inversion, and (c) borehole performed on site.

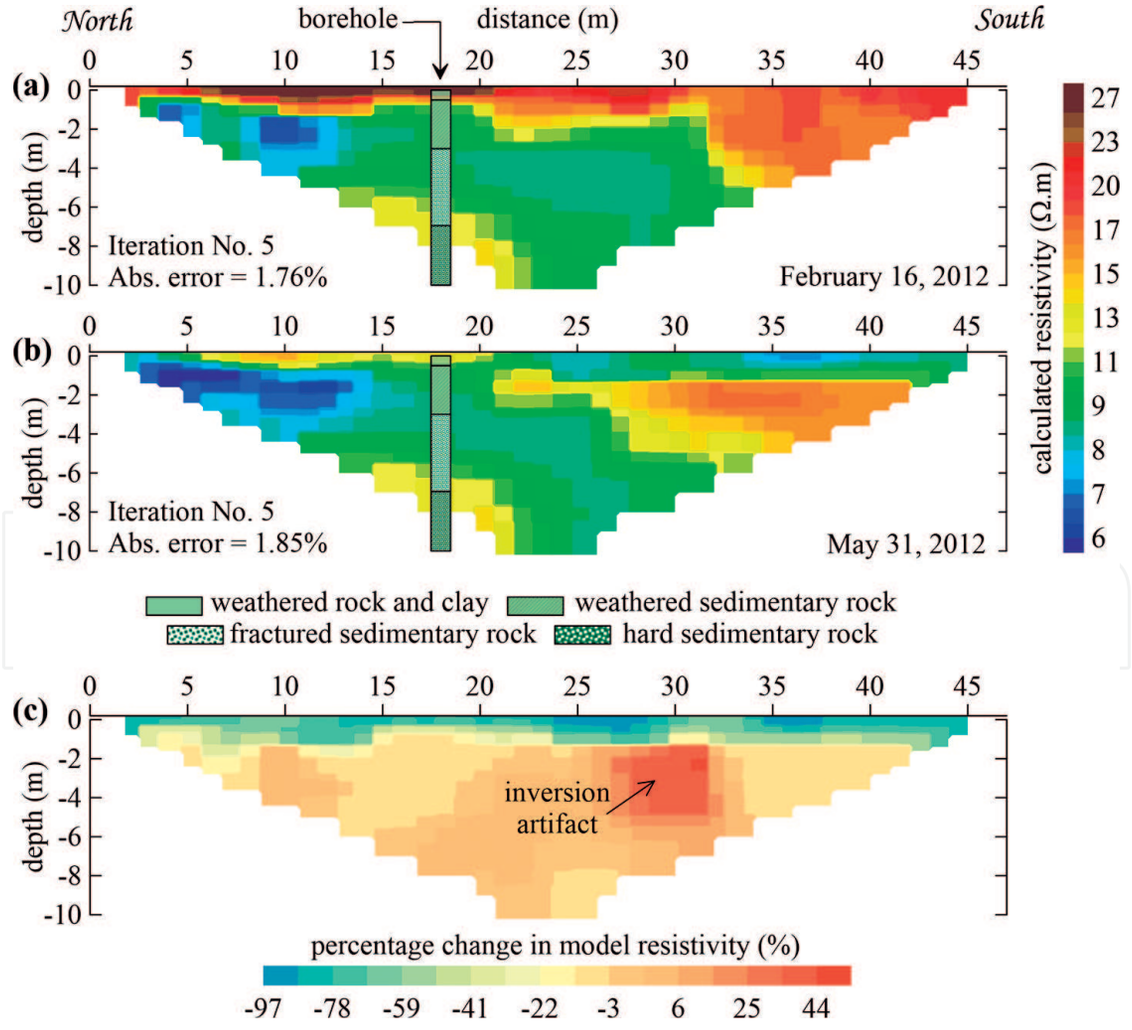


Figure 8. Electrical resistivity tomography obtained for a (a) reference test – February 16, 2012 – and (b) second test, May 31, 2102. (c) Percentage changes in model resistivity obtained in this study.

of calculated electrical resistivity and thickness. After solving the inverse problem for each dataset, the errors obtained were not greater than 2.1%. **Figure 7(b)** shows a three-layer model for each test.

In both cases, the resolution of the inverse problem suggests the existence of a first layer of 14.5–19.7 Ω.m and a variation of thickness from 0.6 m to 1.6; this effect is linked to the change from dry to rainy season. Water-table elevation obtained from a piezometer has shown variation between 1.57 and 0.61 m for each date, followed by a second layer of 8.9 and 9.6 Ω.m and 5.4 and 6.4 m thick for each season, respectively. Finally, there is a last layer with 16.2 and 16.5 Ω.m; the results of this last layer do not show significant changes in their electrical properties and thicknesses. In accordance with the borehole at the site, the two first layers are linked to weathered and fractured sedimentary rock, while the last layer reported for both analyses is linked to hard sedimentary rock.

4.3. Electrical resistivity imaging and time-lapse results

Figure 8(a) and **(b)** show the results of inverse problem solution; in these electrical tomographies, it is possible to identify a first horizon related to weathered rocks and clay (13–27 Ω.m) with tones in brown, red, and yellow. The changes in calculated resistivity values are related to the beginning of rainy season; saturation of surface horizons can produce a decrease in calculated resistivity value. At depth, it is possible to identify a low resistivity (6–13 Ω.m) horizon from the result of **Figure 8(a)**. However, these low values are also revealed at shallow depth; see **Figure 8(b)**. About **Figure 8(c)**, high negative percentage changes are linked to increase of water content in subsoil produced by rains which occurred on May 31, 2012. At depth, the percentage changes are close to 0. Positive percentage changes in model resistivity are related to inversion artifacts. It is possible that these unrealistic changes can be linked to the removal electrode after the first test or inversion scheme used in this analysis.

5. Conclusions

The results of this study show the value of petrophysical relationship of soil samples in understanding the potential function between the electrical properties of rocks and its volumetric water content. These functions can help to understand the evolution of vadose zone moisture in response to seasonal changes in the tropics. Electrical sounding and electrical resistivity imaging are useful tools not only for monitoring changes in the physical properties of this kind of soils but also for associating the different types of soils and rocks with its electrical properties. We have seen the association of these results with the borehole at the site. The strong negative percentage variation in calculated resistivity values presented in the surveyed area shows the important seasonal changes occurring in the tropics, where these negative values are related to the superficial infiltration produced by the rainfall during the transitional season (dry → rainy). The positive percentage changes in model resistivity can be associated with artifacts, linked to inversion method used or due to the removal of the electrodes after each test.

Acknowledgements

I am grateful to the Technological University of Panama and National Research System of SENACYT for all their support. I would like to thank the reviewers for their constructive observations.

Conflict of interest

Author discloses no potential conflicts of interest.

Author details

Alexis Mojica[1,2]*

*Address all correspondence to: alexis.mojica@utp.ac.pa

1 Research Laboratory in Engineering and Applied Sciences, CEI, Technological University of Panama, Panama

2 Tocumen Extension and National Research System, SENACYT, Panama

References

[1] Parasnis DS. Principles of Applied Geophysics. 5th ed. London: Chapman & Hall; 1997. 429 p

[2] Nover G. Electrical properties of crustal and mantle rocks – A review of laboratory measurements and their explanation. Surveys in Geophysics. 2005;**26**:593-651. DOI: 10.1007/s10712-005-1759-6

[3] Telford WM, Geldart LP, Sheriff RE. Applied Geophysics. 2nd ed. New York: Cambridge University Press; 1990. 770 p. DOI: 10.1017/CBO9781139167932

[4] Vogelsang D. Environmental Geophysics. A Practical Guide. 1st ed. Germany: Springer-Verlag; 1995. 173 p

[5] Reynolds JM. An Introduction to Applied and Environmental Geophysics. 2nd ed. Chichester: Wiley; 2011. 710 p

[6] Mussett AE, Khan MA. Looking into the Earth. An Introduction to Geological Geophysics. 1st ed. New York: Cambridge University Press; 2000. 470 p. DOI: 10.1017/CBO9780511810305

[7] Lowrie W. Fundamentals of Geophysics. 2nd ed. New York: Cambridge University Press; 2007. 390 p. DOI: 10.1017/CBO9780511807107

[8] Archie GE. The electric resistivity log as an aid in determining some reservoir characteristics. Transactions of AIME. 1942;**146**:54-62. DOI: 10.2118/942054-G

[9] Grellier S, Bouyé JM, Guérin R, Robain H, Skhiri N. Electrical Resistivity Tomography (ERT) applied to moisture measurements in bioreactor: principles, in situ measurements and results. In: International Workshop Hydro-Physico-Mechanics of Landfills; Grenoble. France. March 21-22, 2005. 5 p

[10] Grellier S, Guérin R, Robain H, Bobachev A, Vermeersch F, Tabbagh A. Monitoring of leachate recirculation in a bioreactor landfill by 2-D electrical resistivity imaging. Journal of Environmental & Engineering Geophysics. 2008;**13**:351-359. DOI: 10.2113/JEEG13.4.351

[11] Jayawickreme D, Van Dam RL, Hyndman DW. Subsurface imaging of vegetation, climate, and root-zone moisture interactions. Geophysical Research Letters. 2008;**35**:5. DOI: 1029/2008GL034 690

[12] Miller CR, Routh PS, Brosten TR, McNamara JP. Application of time-lapse ERT imaging to watershed characterization. Geophysics. 2008;**73**:G7-G17. DOI: 10.1190/1.2907156

[13] Carey AM, Paige GB, Carr BJ, Dogan M. Forward modeling to investigate inversion artifacts resulting from time-lapse electrical resistivity tomography during rainfall simulations. Journal of Applied Geophysics. 2007;**145**:39-49. DOI: 10.1016/J.JAPPGEO.2017.08.002

[14] Mojica A, Díaz I, Ho CA, Ogden F, Pinzón R, Fábrega J, Vega D, Hendrickx J. Study of seasonal rainfall infiltration via time-lapse surface electrical resistivity tomography: Case study of Gamboa Area, Panama Canal Watershed. Air, Soil and Water Research. 2013;**6**:131-139. DOI: 10.4137/ASWR.S12306

[15] Jones SM. Geology of Gatun Lake and vicinity. Geological Society of America Bulletin. 1950;**61**:893-920

[16] Terry RA. A geological reconnaissance of Panama California Academy of Sciences. 1956; **23**:1-91

[17] Woodring WP. Geology and paleontology of Canal Zone and adjoining parts of Panama. Washington: United States Department of the Interior; 1973

[18] Stewart RH, Stewart JL, Woodring WP. Geologic Map of Panama Canal and Vicinity, Republic of Panama. Washington, DC: Department of the Interior, United States Geological Survey; 1980

[19] Allred BJ, Groom D, Ehsani MR, Daniels J. Resistivity methods. In: Allred BJ, Daniels JJ, Ehsani MR, editors. Handbook of Agricultural Geophysics. 1st ed. Florida: Taylor & Francis Group; 2008. pp. 85-108

[20] Loke MH, Acworth I, Dahlin T. A comparison of smooth and blocky inversion methods in 2D electrical imaging surveys. Exploration Geophysics. 2003;**34**:182-187. DOI: 10.1071/EG03182

[21] deGroot-Hedlin C, Constable S. Occam's inversion to generate smooth, two-dimensional models from magnetotelluric data. Geophysics. 1990;**55**:1613-1624. DOI: 10.1190/1.1442813

[22] Loke MH, Barker RD. Practical techniques for 3D resistivity surveys and data inversion. Geophysical Prospecting. 1996;**44**:499-523. DOI: 10.1111/j.1365-2478.1996.tb00162.x

[23] Claerbout JF, Muir F. Robust modeling with erratic data. Geophysics. 1973;**38**:826-844. DOI: 10.1190/1.1440378

[24] Ellis RG, Oldenburg DW. Applied geophysical inversion. Geophysical Journal International. 1994;**116**:5-11. DOI: 10.1111/j.1365-246X.1994.tb02122.x

[25] Loke MH. Time-lapse resistivity imaging inversion. In: Proceedings of the of the 5th meeting of the environmental and engineering geophysical society European section. Em1, Budapest; September 1999. DOI: 10.4133/1.2922877

[26] Loke MH. Electrical imaging surveys for environmental and engineering studies. A practical guide to 2-D and 3-D surveys. Penang, Malaysia. 2010. 151 p

IntechOpen

IntechOpen

IntechOpen